

Photoproduction of Negative Mesons in Deuterium*

D. H. WHITE,† R. M. SCHECTMAN, AND B. M. CHASAN
Cornell University, Ithaca, New York

(Received May 19, 1960)

A 24-in. diffusion cloud chamber filled to 14 atmospheres with tritium-free deuterium gas, operating in a magnetic field of 6 kilogauss, has been placed in the 1040-Mev "hardened" bremsstrahlung beam of the Cornell synchrotron. A total of 310 events of the type $\gamma+d \rightarrow p+p+\pi^-$ have been observed and analyzed. Using the "spectator model," a total cross section has been determined for the reaction $\gamma+n \rightarrow p+\pi^-$ from threshold to 1 Bev, in good agreement with the results obtained from the measurement of the negative-to-positive pion ratio together with the measured cross section for the reaction $\gamma+p \rightarrow n+\pi^+$.

The momentum distribution of the low-energy protons in the laboratory system compares very favorably with the internal

momentum distribution of the deuteron as calculated from the Hulthén or Gartenhaus wave functions. The validity of the spectator model for photons above 200 Mev is experimentally justified, as is expected in consideration of the assumptions of the impulse approximation.

A study of the forward-backward asymmetry of the spectator protons in the laboratory system indicates that above photon energies of 250 Mev, there is a 15% deviation from isotropy, favoring the forward beam direction, indicating that the spectator proton is being "pulled along" with the net forward momentum of the rest of the system, through an average forward momentum transfer of about 10 Mev/c.

INTRODUCTION

A STUDY of the photoproduction of charged mesons through the twin reactions,

$$\gamma+n \rightarrow p+\pi^- \quad (1)$$

[hereafter referred to as ($n-$)], and

$$\gamma+p \rightarrow n+\pi^+ \quad (2)$$

[hereafter referred to as ($p+$)], represents a basic step in the investigation of the elementary particles and their interactions. Assuming that only the meson current contributes to the interaction, the rough equality of these two processes is consistent with the charge symmetry in the final state. However, deviations from simple charge-independence predictions are expected to occur through nuclear recoil terms. These deviations are expected to depend upon the energies, angles, and nature of the coupling of the final state particles.

Reaction ($p+$) has been comprehensively studied over a wide range of energies and angles using liquid hydrogen targets. The study of reaction ($n-$), however, has been given considerably less attention, largely owing to the lack of a condensed neutron target. As it is necessary to use bound neutrons for a target in the study of reaction ($n-$), the use of deuterium is clearly preferable because of its simplicity, low binding energy, and its relatively open structure.

In principle, the analysis of photomeson production in deuterium in terms of free nucleon cross sections could be carried out from a comprehensive analysis of the scattering matrix.¹ However, such a method

requires precise measurements to be made over a wide range of angles and energies. On the other hand, the small interaction cross sections of the photon and final-state particles relative to the deuteron size, and the small magnitude of the deuteron binding energy imply that it is a system for which the "impulse approximation" is valid.² Well above threshold where the final-state exclusion and interference effects become small (for photon energies above 200 Mev), the impulse approximation predictions may be reformulated in terms of the phenomenological "spectator model," according to which the production occurs from only one of the nucleons, the other leaving the interaction with its initial internal momentum. When the presence of the spectator proton is properly taken into account, the photoproduction cross section from the free neutron may be determined.

In attempting to measure the cross section of reaction ($n-$), two experimental approaches can be employed.

(a) Minus-to-plus meson ratio: Here the meson yields of the reactions

$$\gamma+d \rightarrow p+p+\pi^- \quad (3)$$

[hereafter referred to as ($d-$)], and

$$\gamma+d \rightarrow n+n+\pi^+ \quad (4)$$

[hereafter referred to as ($d+$)] are measured and their ratio at a given meson angle and energy is evaluated. It is then necessary to multiply this ratio by the appropriate well-measured differential cross section for reaction ($p+$). This method is the more popular since it is so amenable to counter technique and since, in determining the ratio, most of the deviations from the impulse approximation cancel, as do

* Supported in part by the joint program of the Office of Naval Research and the U. S. Atomic Energy Commission.

† This paper is based on a thesis submitted to the Graduate School of Cornell University in partial fulfillment of the requirements for a Ph.D. degree.

¹ G. Chew and F. Low, Phys. Rev. **113**, 1540 (1959). This method has been used for the analysis of reaction ($d-$) near

threshold by W. P. Swanson, J. D. Anderson, D. C. Gates, T. L. Jenkins, and R. W. Kenney, Bull. Am. Phys. Soc. **5**, 237 (1960).

² G. Chew and H. Lewis, Phys. Rev. **84**, 779 (1951); M. Lax and H. Feshbach, Phys. Rev. **88**, 509 (1952).

most of the experimental systematic errors. However the spectator nucleon momentum distribution smears out the photon spectrum contributing to a well-defined meson energy and angle, and thus creates a problem in resolution, although not a serious one above the threshold region.

(b) The absolute negative meson cross section from the bound neutron: Since reaction (d^-) has three charged particles in the final state, the comprehensive study of this reaction virtually requires a photographic record to be made. The visual technique obviously is limited by the difficulty of poor statistics, but has the advantage in permitting generally unbiased analysis of the entire reaction, and in particular, allows a comprehensive study to be made of the spectator protons. Specifically, the presence of the spectator proton can be taken into account on an event-by-event basis. Moreover, the spectator momentum distribution within the framework of the spectator model provides a direct experimental evaluation of the deuteron momentum wave function, or alternatively, the measured momentum and angular distribution of the spectator protons bears on the validity of the spectator model.

Our experimental approach has been to take stereoscopic pictures of individual events occurring in a deuterium-filled diffusion cloud chamber. The diffusion chamber is particularly suited to the study of the spectator process because of the high deuterium purity, and because the density is sufficiently low that the ow-momentum spectator protons have a measurable range and direction.

APPARATUS

The experimental arrangement is illustrated in Fig. 1. The bremsstrahlung beam of the Cornell synchrotron (peak energy 1040 Mev) was "hardened" by 2.7 radiation lengths of lithium hydride to remove the low-energy photons.³ After being collimated to a

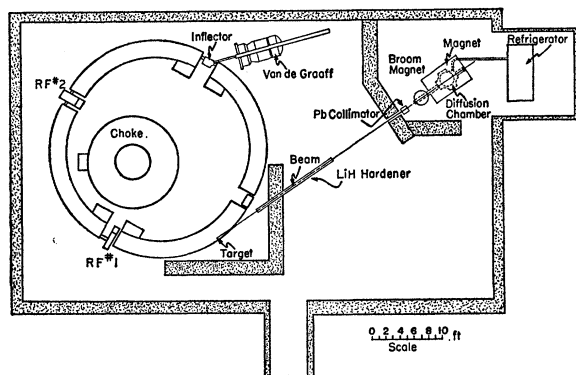


FIG. 1. Arrangement of the synchrotron, cloud chamber, and ancillary equipment.

³ E. L. Hart and D. H. White, Rev. Sci. Instr. 31, 33 (1960).

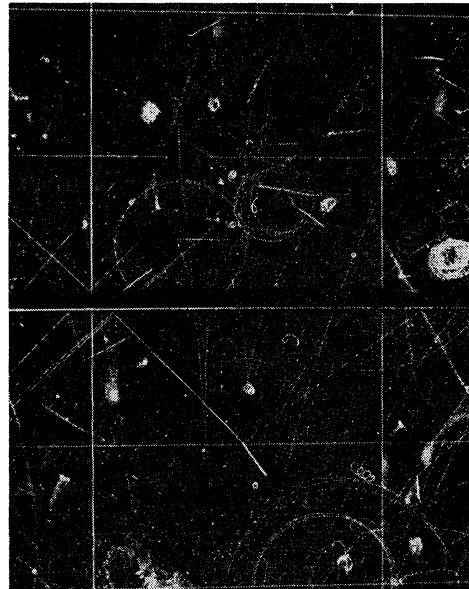


FIG. 2. A sample photograph containing an event of the type $\gamma+d \rightarrow p+p+\pi^-$ produced by a 350-Mev photon. The light track is the negative pion whereas the darker track is a high-energy proton. The dark stopping track is the spectator proton, with about 60 Mev/c momentum.

1-in. by $\frac{1}{2}$ -in. ribbon, the beam is made to traverse the sensitive layer (24 in. diam, 2 in. high) of a diffusion cloud chamber, operating in a magnetic field of 6.1 kgauss, and filled to 20 atm with deuterium. As the β^- activity in commercial deuterium would have created an intolerable background in a diffusion cloud chamber, specially prepared deuterium with a tritium contamination of less than one part in 10^{14} was obtained.⁴ The beam intensity was adjusted to produce no more than about 10 electron pairs per burst, and stereoscopic pictures were taken every 15 seconds.⁵

ANALYSIS

About 28 000 pairs of pictures have been taken, yielding 310 acceptable examples of reaction (d^-), of which an example is shown in Fig. 2. All pictures have been scanned twice, and the resulting scanning efficiency for 3-prong meson events is estimated to be close to 100%. However there are a number of such 3-prong events which may, under certain circumstances, be confused with reaction (d^-). These are:

(a) Multiple meson production: Reactions of the type

$$\gamma+d \rightarrow p+p+\pi^-+\pi^0 \quad (5)$$

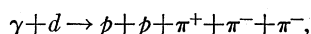
and

$$\gamma+d \rightarrow p+n+\pi^++\pi^- \quad (6)$$

⁴ The deuterium gas with tritium-to-deuterium ratio of 7×10^{-16} was supplied by the Isotope Division of the Oak Ridge National Laboratories.

⁵ A more detailed description of the apparatus and technique may be found in J. M. Sellen, G. Cocconi, V. T. Cocconi, and E. L. Hart, Phys. Rev. 113, 1323 (1959).

are each expected to be about 20% as abundant as reaction ($d-$). These reactions can usually be separated from reaction ($d-$) by detailed kinematic analysis. Moreover, the positive meson in reaction (6) can usually be identified immediately by its light ionization, unless it could be consistent with a high-energy proton. These multiple meson events are presently being analyzed in an independent study.⁶ Multiple meson events of even higher multiplicity are much rarer yet, although two examples of the only 5-prong triple meson reaction,



have been seen. These arguments are not appreciably altered by the presence of similar processes in which the deuteron remains intact. The cross section for production of μ -meson pairs is considered to be negligibly small.

(b) Impurity stars: Under certain circumstances, photon reactions with the gaseous impurities or methyl alcohol vapor can produce a single meson and two heavily ionizing tracks, thus simulating reaction ($d-$). However, most of these can be resolved by detailed kinematic analysis. Moreover, a study of single-meson impurity stars in hydrogen,⁵ in which no confusion is possible, indicates that the number of such events would be of the order of one or two.

There are a fair number of electromagnetic 3-prong events such as neutral meson events in which the π^0 undergoes decay through the 2-electron mode, and electron pair production in which a significant fraction of the incident energy is transferred to the nucleus. These events are easily distinguished by the light ionization and small angle between the electrons.

All the events found were reprojected stereoscopically into space in order to measure directly the pertinent kinematic parameters. In practically all of the events studied, the spherical polar angles with respect to the beam direction could be measured with a precision of about $1-2^\circ$. In principle, the angles above are sufficient for a complete kinematic analysis. However, most of the events were overdetermined by additional measurements such as curvature of sufficiently long tracks, or ranges of stopping protons. Visual ionization estimates were used for particle identification and to corroborate the momentum determinations. In about 40% of the events, the spectator proton stopped in the chamber. However, in about 10% of the events the spectator range was so small that it appeared as a blob, and its direction could not be determined. The combined uncertainties result in an average photon energy resolution of about 10-15%.

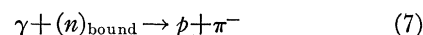
THE TOTAL CROSS SECTION

The energy distribution of the events, together with a knowledge of the photon spectral shape as determined

⁶ R. M. Schectman, B. M. Chasan, and D. H. White, *Bull. Am. Phys. Soc.* **5**, 236 (1960).

from the previous work of Hart,^{3,7} carried out under similar geometry [Fig. 3(a)], permits a cross-section determination to be made. The total number of electron pairs and triplets counted in every tenth picture allows an absolute scaling of the cross section (see reference 5). Assuming 100% scanning efficiency, the total cross section for the reaction ($d-$) is displayed in Fig. 3(b). Below 400 Mev, the statistics are fairly good, whereas for higher energies, the relative errors become progressively larger, since the photon spectrum falls rapidly, resulting in a small fraction of the events occurring above 600 Mev.

Within the framework of the spectator model, the detailed event analysis now permits an event-by-event transformation into the system in which the neutron is at rest. Referring to the photon energy and density as it appears in that system, the total cross section as a function of energy is determined for the reaction



[see Fig. 3(c)]. The identification of the spectator as

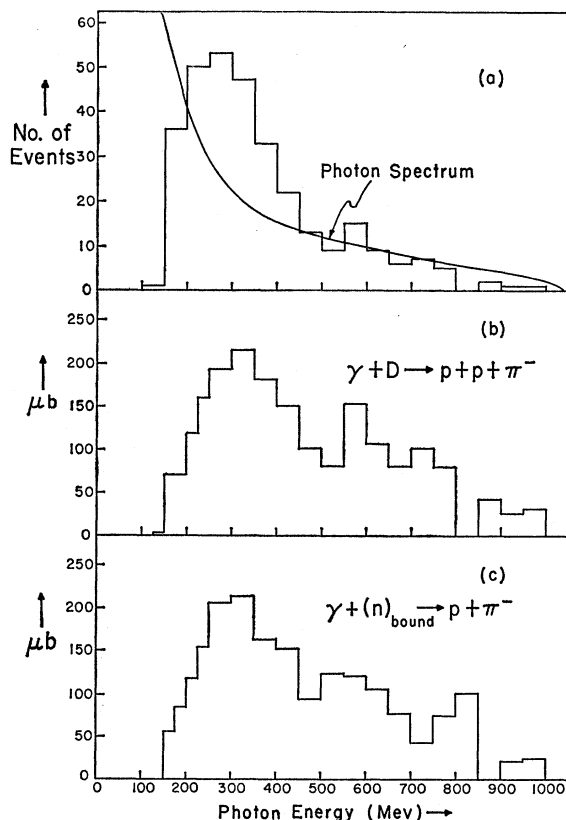


FIG. 3. (a) The histogram represents the energy distribution of the photons responsible for the single-meson events. The curve is the photon spectrum traversing the chamber. (b) and (c). The total measured cross sections for the reactions $\gamma + d \rightarrow p + p + \pi^-$ and $\gamma + (n)_{\text{bound}} \rightarrow p + \pi^-$, respectively.

⁷ E. Hart, G. Cocconi, V. T. Cocconi, and J. M. Sellen, *Phys. Rev.* **115**, 678 (1959).

the lower energy proton is open to question in a number of events (mostly near threshold) where the two proton momenta are comparable. Generally, however, the transformation does eliminate the effects of nucleon motion without loss in resolution.

The free neutron cross section may now be related to the bound neutron cross section through the relation

$$\sigma_n^- = \frac{\sigma_d^-}{\sigma_d^+/\sigma_p^+} \left(\frac{\sigma_d^+/\sigma_p^+}{\sigma_d^-/\sigma_n^-} \right). \quad (8)$$

Since the impulse approximation is valid to first order, it can be argued that the quantity in parenthesis differs from unity only through Coulomb difference effects in the final state. That is, in the case of reaction ($d+$) there are no Coulomb effects, whereas in reaction ($d-$) there is (a) the Coulomb repulsion between the two protons which tends to depress the cross section, and (b) the creation of a negative pion in the field of the two protons, which tends to enhance the cross section. These Coulomb corrections have been evaluated⁸ and only became important below photon energies of 200 Mev. The positive pion deuterium-to-hydrogen ratio has been measured at selected angles and energies by several authors but mostly at low photon energies where the ratio is significantly less than unity. As applied to the denominator of Eq. (8), the values of Beneventano and Penner below 250 Mev⁹ have been used. At higher energies, the approach of this ratio to unity is guided by the cross section for the deuteron photodisintegration

$$\gamma + d \rightarrow p + n, \quad (9)$$

the only significant process competing with reaction ($d-$) in this energy region.¹⁰

Applying the above-mentioned corrections (of order 20% at 200 Mev) to Eq. (8), the total cross section for the free neutron [reaction ($n-$)] is determined (see Fig. 4).

Comparison is now to be made with the results of the minus-plus meson ratio data, through the relation

$$\sigma_n^- = \sigma_p^+ \frac{\sigma_d^-}{\sigma_d^+} \left(\frac{\sigma_d^+/\sigma_p^+}{\sigma_d^-/\sigma_p^-} \right).$$

Below 250 Mev, the results of Beneventano *et al.* have been used, whereas at higher energies, the minus-plus ratio measurements of Sands *et al.*¹¹ and Neugebauer *et al.*¹² are used. The corresponding total cross

⁸ A. M. Baldin, Nuovo cimento 8, 569 (1958); S. Penner, Phys. Rev. 105, 1113 (1957).

⁹ M. Beneventano, G. Bernardini, G. Stoppini, and L. Tau, Nuovo cimento 10, 1109 (1958), Fig. 3.

¹⁰ R. R. Wilson, Phys. Rev. 104, 218 (1956).

¹¹ M. Sands, J. G. Teasdale, and R. L. Walker, Phys. Rev. 95, 592 (1954).

¹² G. Neugebauer, W. D. Wales, and R. L. Walker, Bull. Am. Phys. Soc. 4, 274 (1959); Phys. Rev. Letters 2, 429 (1959); and private communication.

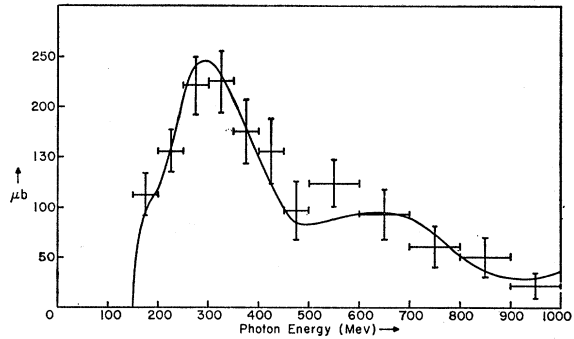


Fig. 4. Measured total cross section for the reaction $\gamma + n \rightarrow p + \pi^-$. Horizontal bars indicate the energy bin-widths, and vertical bars indicate statistical errors only. The curve represents the measured cross section as evaluated from the minus-plus ratio.

section for reaction ($p+$) has been measured extensively throughout the entire energy range.¹³ The resulting function is also displayed in Fig. 4 (solid curve), and it is concluded that within statistics, there is good agreement.

THE MOMENTUM DISTRIBUTION OF THE SPECTATOR PROTON

If one of the nucleons in the deuteron were not involved in the interaction, its laboratory momentum would define its internal momentum. The spectator proton momentum distribution in the laboratory would then be representative of the deuteron momentum density, as evaluated from the momentum wave function of the deuteron $\phi(p)$, i.e.,

$$P(p) = 4\pi(p^2/\hbar^2)\phi^2(p) \\ = 4\pi \left[\int_0^\infty r\psi(r) \sin\left(\frac{p}{\hbar}r\right) dr \right]^2,$$

where $\psi(r)$ is the normalized deuteron position wave function. Although many wave functions have been proposed as a result of various theories and phenomenological models, comparison will be made with distributions calculated from the Gartenhaus and Hulthén wave functions. The Gartenhaus wave function is derived numerically from Yukawa meson theory in second and fourth order with cutoff, and requires a two-parameter fit. The Moravcsik analytic approximation to the S-wave part,

$$\psi(r) = 2.81re^{-1.17r}, \quad r < 2.50f \\ \psi(r) = 1.81r^{-1}(e^{-0.232r} - e^{-1.25r}), \quad r > 2.50f$$

is Fourier-analyzed to determine the momentum

¹³ The pertinent total π^+ cross section at low energies was that as analyzed by M. Moravcsik, Phys. Rev. 107, 600 (1957). Above 250 Mev, the cross section for reaction (1) was used directly from the work of Neugebauer (see reference 12), in which the π^+ cross section was taken from the work of F. P. Dixon and R. L. Walker and older C.I.T. data.

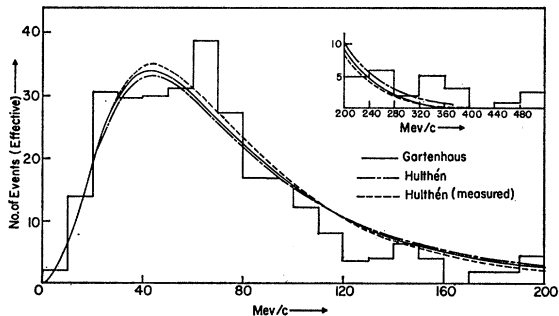


FIG. 5. Histogram of the laboratory distribution of spectator momenta, corrected for cross-section bias. Curves represent internal deuteron momentum distributions as calculated by the Hulthén and Gartenhaus wave function, as well as the Hulthén momentum spectrum with the spectator identity ambiguity and inaccessibility folded in (see text). One event is above 500 Mev/c, and is not shown.

spectrum. The Hulthén wave function,

$$\psi(r) = Kr^{-1}(e^{-\alpha r} - e^{-\beta r}),$$

is an iterative approximation to the wave function corresponding to the Yukawa potential and also requires a two-parameter fit. The quantity α is given by the deuteron binding energy and the nucleon mass:

$$\alpha = (ME_b)^{1/2} = 45.7 \text{ Mev}/c.$$

The parameter β , determined as a compromise fit to effective-range theory and low-energy photodisintegration data,¹⁴ is $\beta = 260 \pm 2 \text{ Mev}/c$. The momentum density corresponding to the Hulthén wave function is

$$P(p) = K' \frac{p^2}{[(p^2 + \alpha^2)(p^2 + \beta^2)]^2}.$$

Comparison of the two calculated spectra indicates that the differences between them are not significant, and for convenience, the Hulthén distribution shall be adopted in subsequent calculations. However, the adjustable parameters of all phenomenological wave functions are determined by low-energy experiments, which are not sensitive to the structure of the deuteron core. Although the low-momentum region and peak position of the various momentum wave functions would then necessarily be essentially the same, the tail would not because of the lack of data concerning nuclear forces at small distances. For instance, the presence of a repulsive core tends to depress the tail appreciably. In spite of the precision with which the parameter β is determined in the Hulthén wave function, the sensitivity affects the over-all normalization rather than the detailed shape of the tail.

Before the laboratory distribution is compared with the calculated spectrum, there are two sources of systematic error which must be considered, aside from the question of experimental resolution and statistics.

The first involves the dependence of the cross section on the initial momentum of the struck nucleon, and hence on the momentum and direction of the spectator. Although the momentum distribution is fairly insensitive to this bias, a correction is made by weighting each event by $\sigma(E)/\sigma(E')$, where $\sigma(E)$ and $\sigma(E')$ are the cross sections in the rest system of the deuteron and neutron, respectively. It must be noted that between photon energies of 145 and 150 Mev the cross section for production from the neutron at rest is zero, whereas from the deuteron it is not. Events in this region occur only if the spectator has a forward nonzero momentum. Even well above threshold, a spectator proton whose kinetic energy is not small with respect to the available energy may prevent the event from occurring, especially if emitted backward, and its absence cannot be properly compensated for. This bias shall be referred to as the "kinematic inaccessibility."

The second source of systematic error is the question of the proper identification of the spectator. As this "ambiguity" is inherent in the spectator analysis, it is necessary to attempt to predict the expected lower-momentum proton distribution *a priori*, based upon an initial Hulthén spectrum. This has been carried out as a Monte-Carlo calculation with the aid of a digital computer. The resulting normalized "measured" distribution, which also includes the effects of the kinematic inaccessibility, is depicted in Fig. 5, and it is this curve with which the experimental data should be compared. The energy dependence of the ambiguity and inaccessibility is tabulated in Table I, and it should be noted from Fig. 5 that the integrated deviation from the correct Hulthén spectrum is not large.

It must be kept in mind that when the two protons have comparable momenta, the violation of energy conservation in the intermediate state is comparable with the interaction energy. Thus, the spectator identification ambiguity as well as the kinematic inaccessibility are symptomatic of a more basic failure in the impulse approximation assumptions, and the classical treatment is no longer valid. The point, then, is that a region of the deuteron momentum distribution is adequately studied within the framework of the

TABLE I. Fraction of events excluded, struck protons incorrectly included, and forward-backward asymmetry in the spectator distribution as determined by a Monte-Carlo calculation for several incident photon energies.

E (Mev)	200	300	400	Above 500	Weighted average
Percent inaccessibility	6.2	0.6	0.1	0.0	4.1
Percent ambiguity	5.5	3.1	2.0	0.4	3.9
Percent forward-backward asymmetry	3.4	0.5	0.0	0.0	2.9

¹⁴ K. S. Suh, Am. J. Phys. 28, 327 (1960).

spectator model only if the available energy is large with respect to the momentum region of interest.

The corrected spectator laboratory momentum distribution based on 310 events is depicted in Fig. 5. The fit to the calculated internal momentum distribution is generally good. The apparent flattening of the peak must be attributed to statistical fluctuation, as the momentum resolution in this region is less than 4 Mev/ c since most of the spectators are stopping. Above 60 Mev/ c , the resolution is about 10–15%. As the energies involved in the photoproduction interaction are generally large with respect to the internal energy, final-state interactions would be expected on the average to increase the spectator momenta, and the tail of the spectator momentum distribution should appear raised at the expense of the lower energy peak. Although the slight shift of the experimental peak of higher energies may not be statistically significant, there are 10 spectator protons above 320 Mev/ c , most of which must be interpreted as having interacted. On the other hand, the region from 80 to 240 Mev/ c is consistently less populated than expected and cannot be accounted for by the small surplus above 240 Mev/ c . If the momentum wave function is correct, this suppression must be due to the competing photodisintegration reaction which would be important when the nucleons are close together at the time of interaction, and therefore have high relative momentum. The separation of these two competing effects involves the independent calculation of one of them, i.e., the photodisintegration probability as a function of nucleon separation. On the other hand, at the higher photon energies (above 500 Mev), photodisintegration ceases to be of importance, and the deviations of the experimental distribution from the true spectrum must occur essentially through final-state interactions. Moreover, at this energy the biases arising from ambiguity and inaccessibility are negligibly small.

Referring to Table II, it is clear that for spectator momenta not small with respect to the available energy, the spectator density is suppressed as expected, owing mostly to the kinematic inaccessibility mentioned earlier. For high-energy photons, the spectator momen-

tum region above 240 Mev/ c is quite highly populated, at the expense of the 80–240 Mev/ c region. The results in this region may be partially vitiated by the possible contamination of a few misidentified meson pair events and by the degeneration in momentum resolution. However, most of these events should be correctly classified and an interpretation of this feature may be that when the two nucleons are in an initial high relative momentum configuration and are therefore close together, the spectator proton has a good chance of becoming involved in the interaction. The nature of this interaction would be difficult to evaluate within the framework of the impulse approximation, but some pertinent ideas will be discussed in the following section.

THE ANGULAR DISTRIBUTIONS

In the search for the presence of final-state spectator interactions, it is appropriate to study possible angular correlations of the spectator proton with the other particles involved, within the capabilities of the statistics.

Such an analysis as this should be carried out within the context of a specific model. For photon energies below 200 Mev, the calculations of Baldin⁸ and the experimental results and analysis of Adamovich¹⁵ represent the most advanced progress in the search for the presence of final-state interactions. Since it is not profitable to analyze threshold photoproduction within the framework of the spectator model, this analysis was carried out under the impulse approximation in terms of the total and relative nucleon momenta.

Baldin's resulting functions, sensitive to final-state interactions, clearly demonstrate that the distribution of the relative nucleon momentum with respect to the total nuclear momentum should be considerably smaller than expected with no final-state interaction. This fact, as verified by Adamovich, indicated that near threshold the protons are positively correlated, i.e., leave the interaction together, as is consistent with a spin-flip interaction, leaving the nucleons in a relative S state. Figure 6, displaying the forward-backward asymmetry of the spectator protons with respect to the photon direction,¹⁶ strongly reflects the proton-proton interaction, which gives preference to the forward direction. Although the Monte-Carlo calculation indicates that the forward-backward asymmetry is not significantly biased by the spectator ambiguity, the kinematic inaccessibility does adversely affect backward emission of the spectator at low photon energies, and the resulting expected bias (see Table I) is included

TABLE II. Fraction of spectator protons in specified momentum bins, grouped in selected photon energy intervals, as compared with that expected from calculations with no final state interaction included.

Spectator momentum range (Mev/ c)	Photon energy interval (Mev)		
	150–230 (65 events)	230–500 (189 events)	500–1000 (55 events)
0–80	77.1±11% (69% calc)	65.5±6% (61% calc)	52.1±9% (60% calc)
80–240	22.9±6% (31% calc)	31.5±4% (37% calc)	22.2±6% (37% calc)
>240	0 (0 calc)	3.0±1.5% (1.7% calc)	25.7±7% (2.7% calc)

¹⁵ M. I. Adamovich, G. V. Kuz'micheva, V. G. Larionova, and S. P. Kharlamov, *J. Exptl. Theoret. Phys. (U.S.S.R.)* **35**, 27 (1959) [*Soviet Phys.-JETP* **8**, 21 (1959)]; and M. I. Adamovich, *J. Exptl. Theoret. Phys. (U.S.S.R.)* **35**, 39 (1958) [*Soviet Phys.-JETP* **8**, 29 (1959)].

¹⁶ In graphs involving angular distributions of the spectator protons, all events with protons of momentum less than 30 Mev/ c have been rejected since their short range results in a loss in angular resolution.

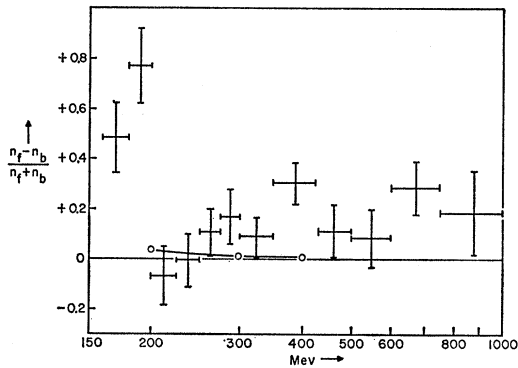


FIG. 6. Forward-backward asymmetry of spectator protons of momentum greater than 30 Mev/c, as a function of incident photon energy.

in Fig. 6. The sharpness of the break at 200 Mev is not to be taken too seriously, although the correlation should rapidly vanish above this value.

Above 200 Mev, no work has been done on the strength of final-state interactions. However, according to Table I, the confidence with which the spectator can be correctly identified enables one to look for possible correlations with the other particles from a more classical approach. A study of the longitudinal projection of the spectator momentum (see Fig. 7), as compared with the Monte-Carlo calculation for no final-state interaction, indicates that, in addition to a handful of unusually high-energy forward spectator protons, there is also a small forward momentum transfer to a large fraction of the spectators. In the light of the latter feature, the 15% forward-backward asymmetry in Fig. 6 may be interpreted as an average forward momentum transfer of about 10 Mev/c to the spectator protons for photon energies from 250 to 1000 Mev.

In spite of the lack of a specific model for high-energy final-state interactions, it seems reasonable that, in the presence of some sort of a final-state interaction, the spectator proton tends to be "pulled along" with the net forward momentum of the rest of the system. It should be noted that this is a small effect in that the relative transfer of forward momentum to the spectator varies from about four percent for photon energies of 300 Mev to about one percent at 1000 Mev.

Considering now the possible sources of interactions that may be responsible for the anisotropy, the photon is the least likely candidate as the magnitude of the nuclear Compton effect is known to be quite small. The proton-proton total cross section together with the laboratory energy distribution of struck protons yields an average cross section of about 50 mb for the protons above 200 Mev/c. The average pion-proton total cross section is about 25 mb. Now the emission of the struck proton is kinematically limited to the forward direction (about 75% are emitted at less than 45° from the beam direction) whereas the pions can be emitted

at all angles, although there is a 60% preference for forward-emitted pions, and moreover the forward pions on the average have higher momenta. Since the 10-Mev/c forward momentum transfer does not seem to be concomitant with a much larger increase in the total momentum (Fig. 5), it must be concluded that the momentum transfer is primarily forward. This conclusion is consistent with the fact that the proton-proton elastic cross section is large with respect to the pion-proton cross section, especially at small proton momenta. A more quantitative calculation, if this classical picture is valid at all, would require a knowledge of the dependence of the interaction probability on the spectator momentum. Alternatively, a correlation of the relative proton angles would be meaningless unless carried out within the framework of a specific model. At high proton energies where the initial spectator momentum is expected to be small with respect to the struck-proton momentum, the events in which the two protons interacted are expected to display a laboratory proton-proton angle distributed close to 90°. Although the angular distribution of the spectator protons of momentum greater than 320 Mev/c has a slight preference for the forward beam direction, the relative proton-proton angles are almost all greater than 120° and are therefore incompatible with p - p scattering. However, the increasing pion-nucleon cross section at these high energies indicates that many of these events are probably a result of pion scattering.

In the absence of a more erudite model, the angular correlations seem to indicate that the 10-Mev/c average forward momentum transfer probably arises from proton-proton interactions at low momentum, whereas the rarer high momentum transfers may be attributed to pion-proton scattering.

CONCLUSIONS AND ACKNOWLEDGMENTS

The use of the diffusion cloud chamber in the study of the spectator process has enabled the three-body interaction to be studied over a wide range in energies.

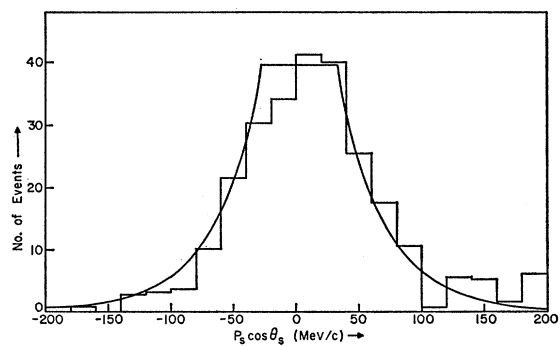
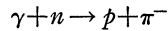


FIG. 7. Longitudinal momentum distribution of spectator protons of momentum greater than 30 Mev/c. Calculated spectrum is that expected from the Hulthén momentum spectrum shifted 2.9 Mev/c to take into account the spectator ambiguity and inaccessibility effects (see text).

The tenuous sensitive medium has made possible the momentum analysis of over 95% of the spectator protons, although the short sensitive height is detrimental, especially as it affects curvature measurement.

The bulk of the useful information in this experiment comes from photon energy region from 200 to 500 Mev. The conclusions may be summarized as follows:

- (a) The total cross section for the reaction



is in good agreement with that determined from the minus-plus pion ratio in deuterium, although the statistics attainable make the latter approach superior above the threshold region.

(b) For photon energies between 200 and 500 Mev, the spectator momentum distribution indicates that the spectator model is quite good, as is expected from consideration of the assumptions of the impulse approximation, and the use of this model in the analysis of meson photoproduction from deuterium in terms of free-nucleon cross sections is clearly justified. Above 500 Mev, there seems to be an increase in the number of high-momentum spectators, although the lack of statistics in this region, together with the attrition of the energy and momentum resolution and a possible contamination of charged meson pair events, makes it difficult to evaluate this effect.

(c) The shape of the spectator proton momentum distribution may be predicted quite well from either the Hulthén or Gartenhaus deuteron wave functions. An apparent suppression of the tail of the experimental distribution may be attributed in part to a competing photodisintegration process or to an actual suppression of the momentum wave function for large momenta, both these features being intimately connected with the question of nuclear forces at small distances. Moreover, the possible presence of final-state interactions as well as the validity of the impulse-approximation assumptions are factors of importance in this region.

(d) There is a forward-backward asymmetry of the spectator proton, with respect to the beam direction, of about 15% for all photon energies above 250 Mev. As this amounts to an average momentum transfer of about 10 Mev/ c , it may be called a small effect.

We would like to express our gratitude to Professor Giuseppe Cocconi and Professor V. T. Cocconi for the instigation of this experiment and their assistance during the early stages. Their contribution, as well as that of Dr. E. Hart, in the development and operation of the cloud chamber and optical equipment is greatly appreciated. We also wish to thank Mrs. Judith Sarfatt, Mrs. Louise Van Nest, and Mrs. Jean Malamud for scanning the large majority of the film.

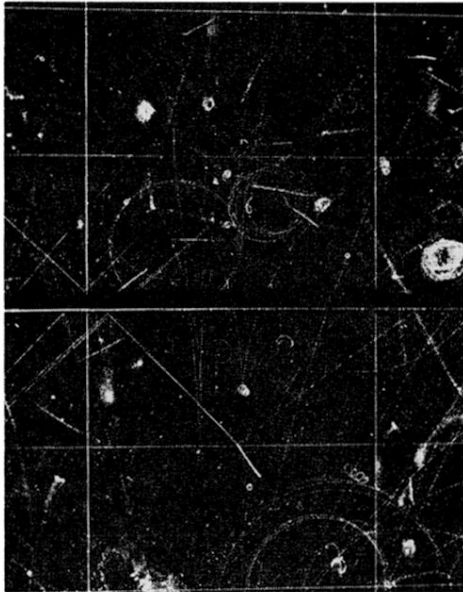


FIG. 2. A sample photograph containing an event of the type $\gamma+d \rightarrow p+p+\pi^-$ produced by a 350-Mev photon. The light track is the negative pion whereas the darker track is a high-energy proton. The dark stopping track is the spectator proton, with about 60 Mev/c momentum.